



# **Spatial Assessment of Agricultural Vulnerability to Climate Change Using MODIS-Derived Satellite-Based Aridity Index (SbAI): A Case Study of Mandya District, Karnataka**

<sup>1</sup>Radhamani V B, <sup>2</sup>Dr. Vishwanatha S, <sup>3</sup>Prof. Chandrashekara B<sup>c</sup>.

<sup>1</sup> Research scholar DOS in Geography, University of Mysore, Mysuru-570006

<sup>2</sup> Teaching Faculty, DOS in Geography, University of Mysore, Mysuru-570006

<sup>3</sup> Senior Professor, DOS in Geography, University of Mysore, Mysuru-570006

## **Abstract**

Climate change poses a significant threat to agricultural sustainability, particularly in semi-arid regions like southern India. This study presents a spatial assessment of agricultural vulnerability to climate change in Mandya district, Karnataka, using a Satellite-based Aridity Index (SbAI) derived from MODIS remote sensing datasets and precipitation data from the PERSIANN system. The SbAI was computed by integrating land surface temperature (LST), broadband albedo, and absorbed solar radiation over a 20-year period (2001–2021). Mandya district, a predominantly agrarian region located in the Cauvery basin, was selected due to its climate sensitivity and dependency on monsoon rains. Spatial and temporal analysis of SbAI revealed significant intra-district variations in aridity, with certain taluks exhibiting increasing arid trends over time. The results showed a gradual intensification of drought-like conditions, especially in the central and southern parts of the district. The study also employed NDVI-based vegetation indices to cross-validate the SbAI findings and identified areas with high vulnerability to climate stress. This spatial approach offers a cost-effective, scalable framework for identifying vulnerable agricultural zones, which can inform targeted interventions and adaptive policy frameworks to mitigate the impacts of climate change on regional food security.

**Keywords:** Aridity Index, Climate Change, MODIS, Agricultural Vulnerability, Mandya, Remote Sensing, NDVI, SbAI

## 1. Introduction

Agriculture is inherently sensitive to climatic variations, and in recent decades, the frequency and intensity of climate-related extremes—such as droughts, floods, and temperature anomalies—have profoundly impacted agricultural productivity, particularly in developing countries (IPCC, 2022). Climate change exacerbates existing vulnerabilities in agrarian communities, threatening food security, rural livelihoods, and sustainable development goals (FAO, 2021). In this context, assessing the spatial dimensions of agricultural vulnerability is crucial for developing targeted adaptation strategies and informed policy responses.

Vulnerability, in the context of climate change, is a function of three key components: exposure to climatic hazards, sensitivity of the agricultural system, and its adaptive capacity (Turner et al., 2003; IPCC, 2014). Spatially explicit assessment allows researchers and policymakers to identify geographic hotspots where agriculture is most at risk, considering both bio-physical and socio-economic parameters (Adger, 2006; de Sherbinin et al., 2019). This is especially pertinent in regions with high environmental variability and socio-economic disparities, where uniform policy interventions often fail to address local complexities.

Recent advances in geospatial technologies and data availability, including satellite remote sensing and Geographic Information Systems (GIS), have enabled comprehensive vulnerability assessments at multiple spatial scales (Malczewski, 2006; You et al., 2020). These tools facilitate integration of multi-dimensional datasets—such as land surface temperature, rainfall variability, soil characteristics, cropping patterns, and demographic indicators—into composite vulnerability indices (Mondal & Tatem, 2012; Pandey et al., 2019). In particular, the use of weighted overlay analysis, Principal Component Analysis (PCA), and Analytical Hierarchy Process (AHP) methods has gained prominence for quantifying vulnerability with spatial precision (Kogo et al., 2020).

Despite the growing body of literature, many existing assessments are limited in spatial resolution or lack integration of both climatic and socio-economic variables. Furthermore, the dynamic nature of vulnerability under projected climate change scenarios necessitates continuous refinement of methodological frameworks. Therefore, this study aims to conduct a spatial assessment of agricultural vulnerability to climate change using an integrated geospatial approach, combining remote sensing data, climate variables, and socio-economic indicators. By mapping vulnerability hotspots, this study seeks to support localized adaptation planning and improve climate resilience in agricultural systems.

The primary objective of this study is to assess the spatial patterns of agricultural vulnerability to climate change by employing the Aridity Index (AI) as a core climatic indicator. The Aridity Index, defined as the ratio of mean annual precipitation to mean annual potential evapotranspiration (UNEP, 1992), serves as a reliable proxy for understanding the moisture availability essential for crop growth. Regions with lower AI values indicate drier conditions and thus higher vulnerability, particularly for rain-fed agriculture. By integrating the AI with spatial datasets such as land use/land cover (LULC), soil types, and agricultural dependency, the study aims to generate a vulnerability map that highlights zones at greater risk due to increasing aridity trends. This approach is particularly relevant for the selected study area, which exhibits a high degree of climatic variability and is predominantly agrarian. Through geospatial analysis, the research

seeks to identify critical zones where adaptive interventions are urgently needed to mitigate the adverse impacts of climate-induced water stress on agricultural systems.

## 2. Study Area

The present study focuses on Mandya district, located in the southern part of Karnataka, India, lying between 12°13' N to 12°49' N latitude and 76°19' E to 77°04' E longitude. The district covers an area of approximately 4,961 square kilometers and is part of the Southern Dry Zone of Karnataka. Mandya is bounded by the districts of Mysuru to the south and west, Tumakuru to the north, and Ramanagara to the east. The district comprises seven taluks—Mandya, Maddur, Malavalli, Pandavapura, Srirangapatna, Nagamangala, and Krishnarajpet—each exhibiting varying agro-climatic conditions. The terrain is predominantly flat with undulating topography in parts, and the average elevation ranges between 600 and 900 meters above sea level.

Mandya is widely recognized as an agriculturally dominant district, often referred to as the "Sugar Bowl of Karnataka" due to its extensive sugarcane cultivation. The agricultural system in the district is heavily reliant on both canal irrigation—primarily from the Krishna Raja Sagara (KRS) dam on the Cauvery River—and seasonal rainfall. However, in recent years, Mandya has experienced increasing climatic variability, including delayed monsoons, erratic rainfall distribution, and prolonged dry spells. Such changes have led to growing concerns over water stress and declining crop productivity, especially in rain-fed areas. Given its economic dependence on agriculture and its exposure to hydrological uncertainty, Mandya presents an ideal case for assessing agricultural vulnerability through the Aridity Index (AI). This study aims to spatially analyse variations in aridity across the district to identify vulnerability hotspots and support climate-resilient agricultural planning.

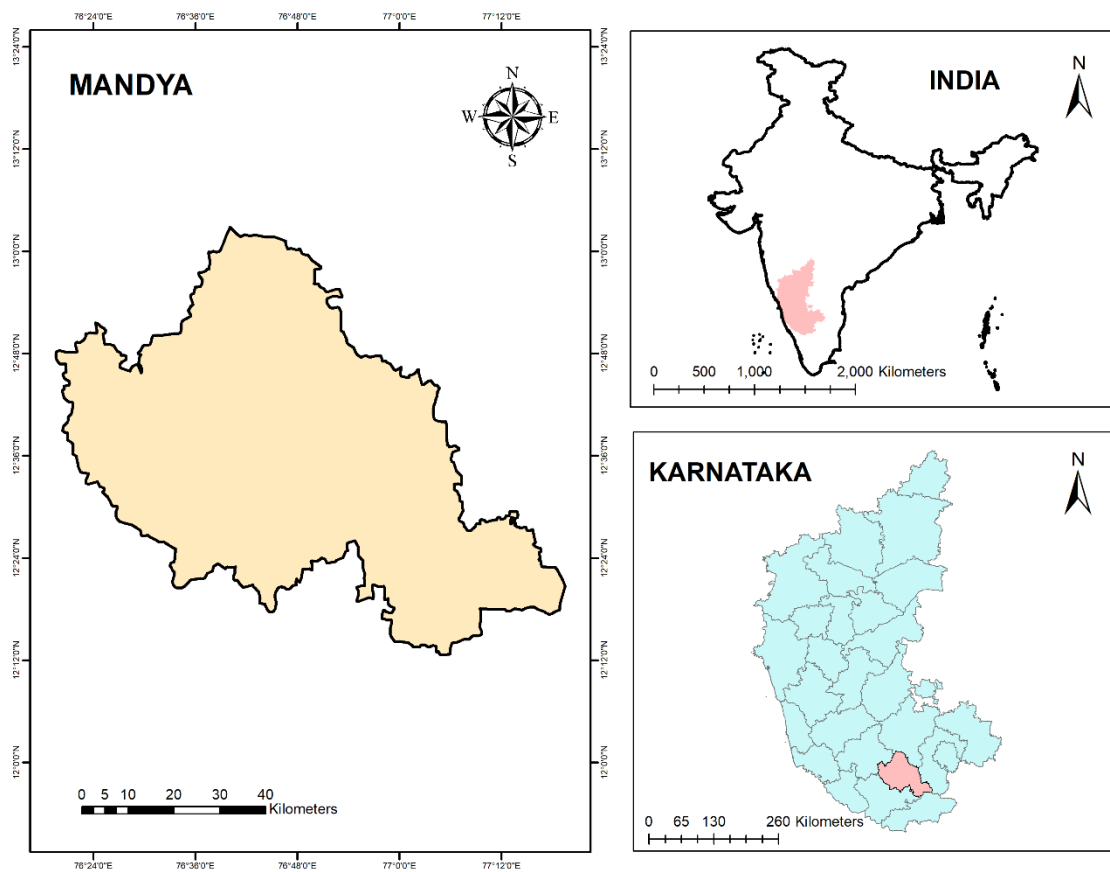


**Figure 1:** Location of the study area

### 3. Data and Methodology

This study utilizes a remote sensing-based approach to calculate the Satellite-based Aridity Index (SbAI) for assessing the spatial and temporal variability of agricultural vulnerability in Mandya district, Karnataka. SbAI serves as an effective proxy to characterize arid conditions by integrating remotely sensed parameters such as Land Surface Temperature (LST), surface albedo, and absorbed solar radiation. The MODIS (Moderate Resolution Imaging Spectroradiometer) satellite products were the primary data source for deriving thermal and reflectance-based variables, whereas precipitation estimates were obtained from the CHIRPS/PERSIANN remote sensing dataset. These datasets were selected for their high temporal resolution, global coverage, and suitability for long-term climate analysis.

The MODIS products used include MOD11A1 (daily LST – daytime), MOD11A2 (8-day LST – nighttime), and MOD09A1 (8-day Surface Reflectance), all having a spatial resolution of 1 km. The data was acquired for a 20-year period (2001–2021) from NASA Earth Data and USGS Earth Explorer portals. The PERSIANN precipitation dataset, with a spatial resolution of approximately 0.25° (25 km) and temporal coverage from 2000 onward, was sourced from the CHRS Data Portal. The geographic extent of Mandya district was delineated using district boundary shapefiles, and subsetting of satellite scenes was performed using ERDAS Imagine. All datasets were reprojected to UTM Zone 44N to ensure spatial consistency for geospatial analysis.

The first step in SbAI calculation involved estimating the diurnal temperature range ( $\Delta T_s$ ) by subtracting nighttime LST from daytime LST:

$$\Delta T_s = \text{LST}_{\text{Daytime}} - \text{LST}_{\text{Nighttime}}$$

This temperature variation is a critical indicator of surface moisture availability and energy fluxes. Subsequently, broadband albedo ( $\alpha$ ) was computed from MODIS surface reflectance data (MOD09A1). This involved calculating vegetation indices such as the Normalized Difference Vegetation Index (NDVI) and Soil Adjusted Vegetation Index (SAVI), which were used as intermediate indicators of vegetation health. NDVI was calculated using the equation:

$$\text{NDVI} = (\text{Band 2} - \text{Band 1}) / (\text{Band 2} + \text{Band 1})$$

while SAVI was derived using:

$$\text{SAVI} = [(\text{Band 2} - \text{Band 1}) \times (1 + L)] / (\text{Band 2} + \text{Band 1} + L)$$

where  $L = 0.5$  to account for soil brightness. These vegetation indices were further used in empirical models to calculate broadband albedo based on a linear combination of MODIS spectral bands using the equation:

$$\alpha = c_1 \times \text{Band1} + c_2 \times \text{Band2} + \dots + c_7 \times \text{Band7}$$

The coefficients ( $c_1$  to  $c_7$ ) were derived from established empirical relationships.

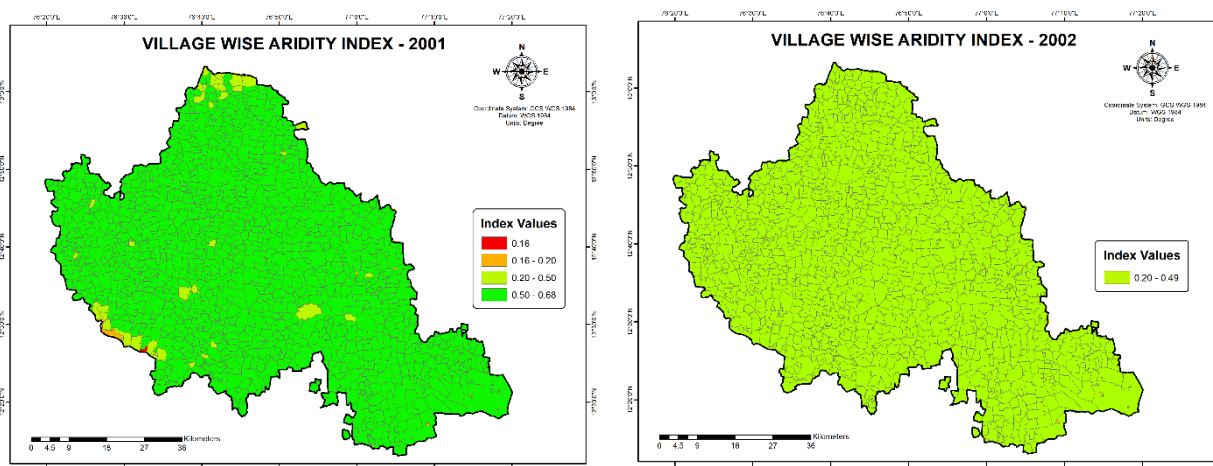
Using the derived albedo, absorbed solar radiation ( $R_s$ ) was estimated with the formula:

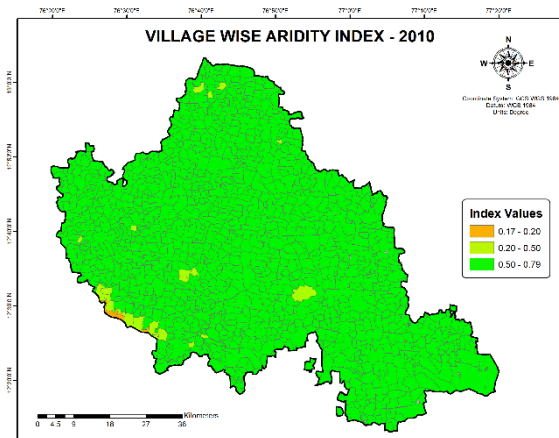
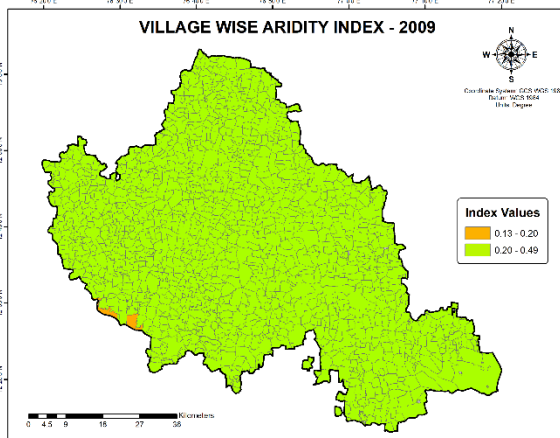
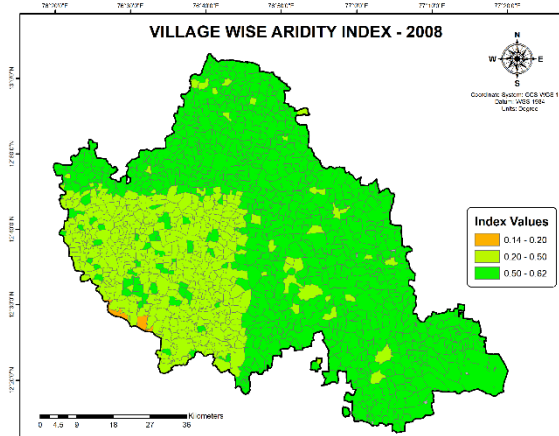
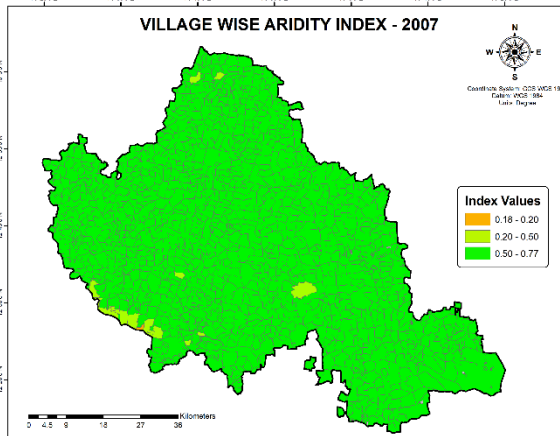
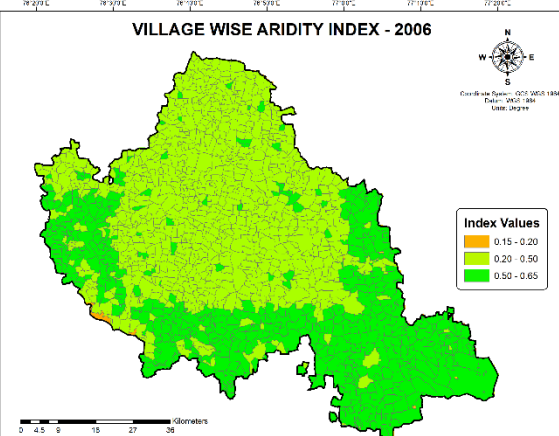
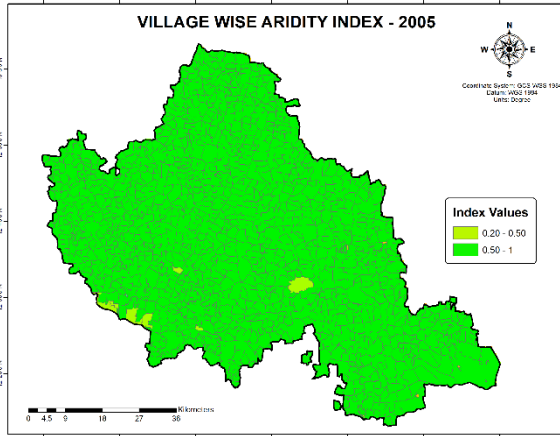
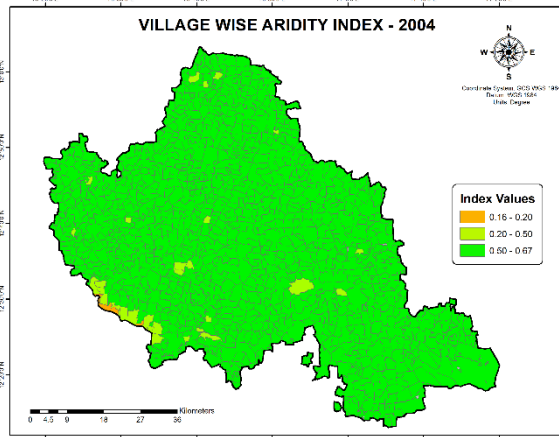
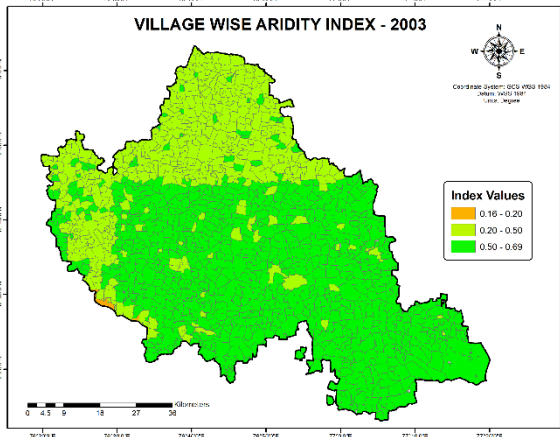
$$R_s = S_0 \times (1 - \alpha)$$

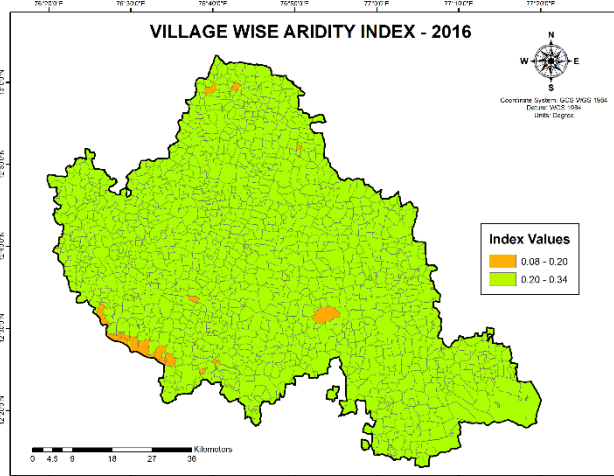
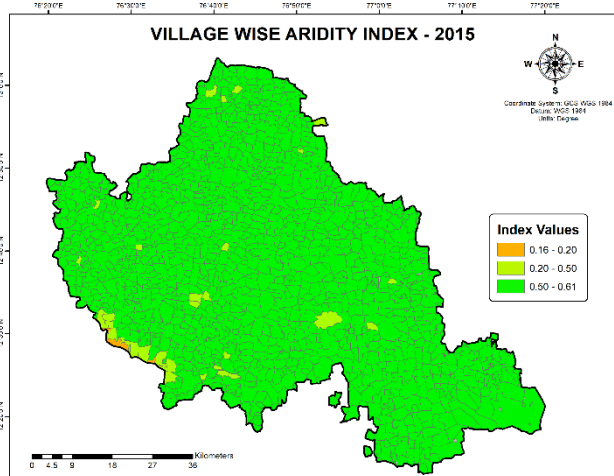
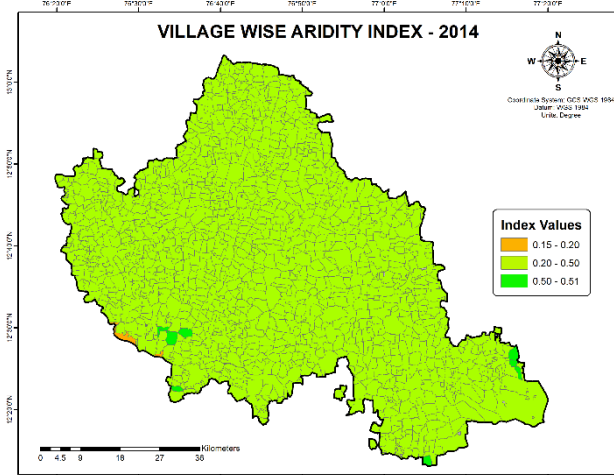
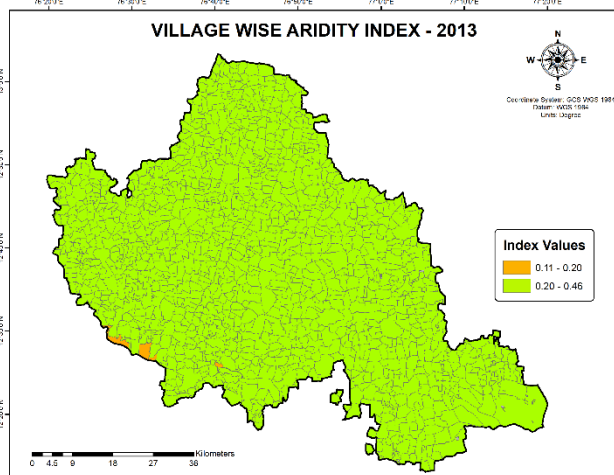
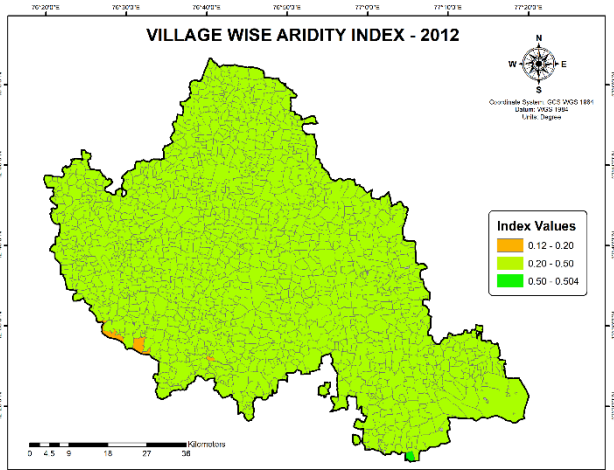
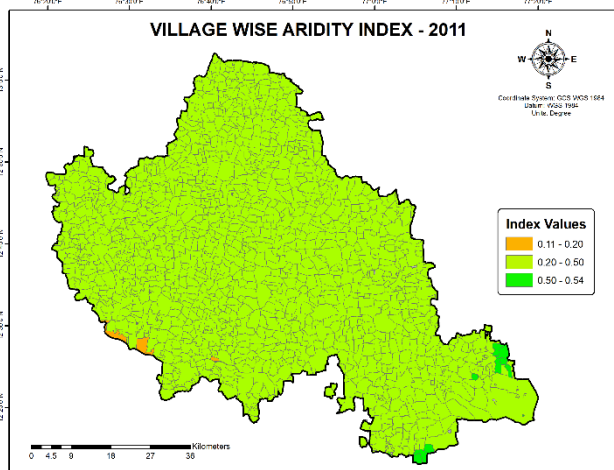
where  $S_0$  is the solar constant, taken as  $1367 \text{ W/m}^2$ . Finally, the Satellite-based Aridity Index (SbAI) was computed as:

$$\text{SbAI} = \Delta T_s / (R_s \times K)$$

Here,  $K$  is an empirical calibration coefficient that varies with vegetation cover and climatic zone. Based on the moderate summer and winter conditions of Mandya (with temperature ranges between  $20^\circ\text{C}$  to  $35^\circ\text{C}$ ), a  $K$  value of 1.4 was selected, aligning with literature-based recommendations for semi-arid subtropical regions.







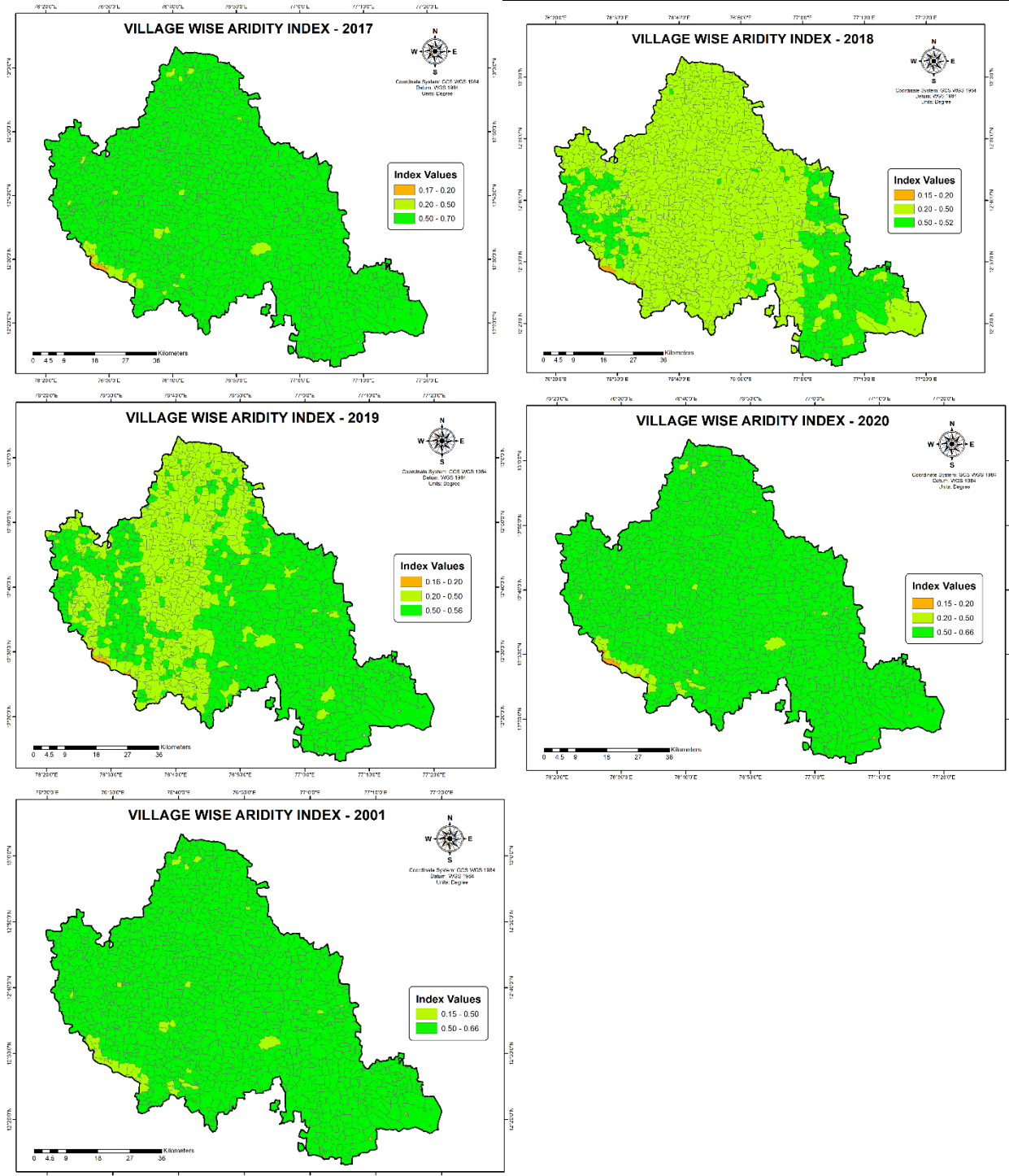


**Figure 2:** Village wise aridity index of Mandya from the year 2001 to 2021

The computed SbAI values were visualized and analysed at the village level using ArcGIS. Spatial analysis involved generating thematic maps to identify high and low aridity zones across Mandya. For temporal analysis, SbAI values were aggregated and compared for the years 2001 and 2021 to understand long-term aridity trends and potential drought patterns. Further, statistical metrics such as mean, standard deviation, minimum, and maximum values of SbAI were calculated for each village to evaluate intra-district variability. Villages exhibiting consistently high aridity values were identified as vulnerable hotspots requiring climate-resilient planning and water management interventions.

Lastly, to enhance the reliability of the results, ground-truth validation was performed by comparing SbAI outputs with field data collected through surveys, including farmer-reported drought experiences and irrigation status. This step ensured that satellite-derived estimates corresponded well with actual agricultural conditions

on the ground, thereby increasing the practical utility of the SbAI as a decision-support tool in regional climate vulnerability assessments.

#### **4. Results and Discussion**

The results of this study present the spatial and temporal variations in aridity across Mandya district over a 20-year period (2001–2021) based on the Satellite-based Aridity Index (SbAI). This index, derived from MODIS LST and reflectance data combined with PERSIANN precipitation, effectively captures surface dryness and moisture stress at the village level. The outcomes are interpreted through spatial maps, temporal graphs, and statistical summaries.

##### **4.1. Spatial Distribution of SbAI (2021)**

The spatial SbAI map for the year 2021 reveals significant heterogeneity in aridity conditions across Mandya district. The SbAI values range from 0.0015 to 0.018, where higher values indicate greater aridity. Villages in the eastern and northeastern taluks, such as Malavalli, Maddur, and parts of Nagamangala, showed relatively higher SbAI values, indicating higher surface dryness and potential vulnerability to agricultural drought. These areas correspond to zones with shallow red soils, lower irrigation coverage, and reduced vegetation cover, as confirmed through land use and NDVI overlays.

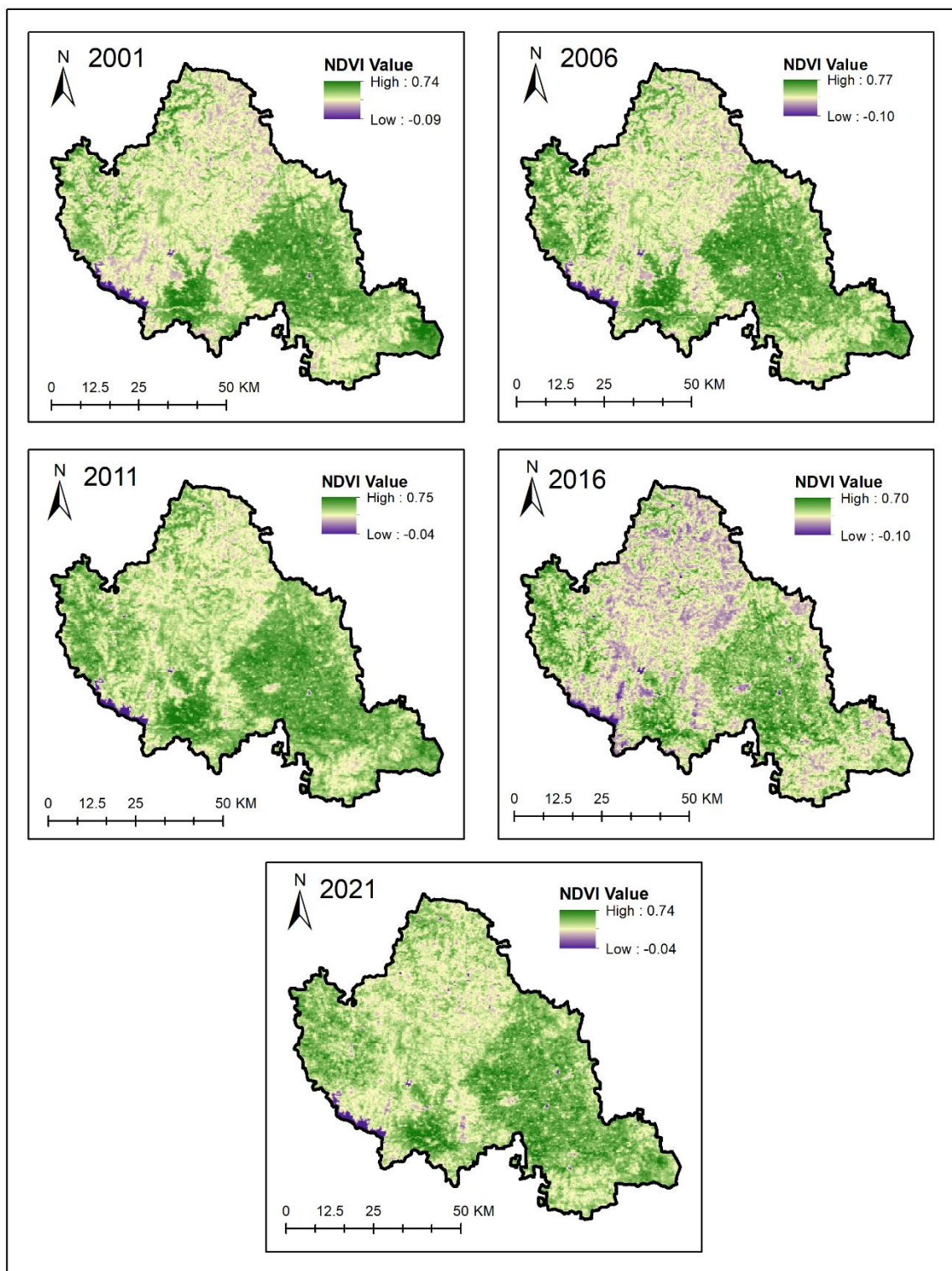


**Figure 3:** NDVI of Mandya district for the study period 2001-2021.

In contrast, villages in Srirangapatna and Pandavapura taluks, particularly those closer to the Cauvery River and canal-fed command areas, displayed lower SbAI values, indicating lesser climatic stress. This spatial pattern reflects the influence of hydrological infrastructure, soil moisture retention, and irrigation accessibility in mitigating surface aridity. The thematic maps clearly delineate vulnerability hotspots, which can serve as a planning tool for prioritizing climate-resilient interventions such as micro-irrigation, watershed management, and drought-tolerant crop planning.

## 4.2. Temporal Changes in SbAI (2001 vs. 2021)

A comparison between SbAI maps of 2001 and 2021 shows a notable increase in aridity levels across the district, with the mean SbAI value increasing from 0.0071 in 2001 to 0.0116 in 2021. This rise suggests an overall drying trend likely influenced by increasing temperatures, decreasing rainfall reliability, and land degradation. The standard deviation also increased, indicating growing spatial disparity in moisture availability and climate impacts across villages.

The most significant increase in aridity was observed in Malavalli and Maddur, which are known to be predominantly rain-fed and have witnessed groundwater depletion and land use shifts towards monoculture. Some villages, like Belakavadi and Kirugavalu, that previously exhibited moderate aridity have transitioned into high-risk zones over the two decades. On the other hand, a few irrigated villages near Mandya town and Srirangapatna showed marginal or no increase, highlighting the buffering effect of water resource infrastructure.

## 4.3. Statistical Summary and Village-Level Trends

Village-wise statistical analysis revealed that out of approximately 700 villages in Mandya, over 200 villages (28%) showed high SbAI values ( $>0.015$ ) in 2021, placing them in the category of severely arid or vulnerable to agricultural drought. The mean SbAI across the district was 0.0116, with minimum values of 0.0015 (in well-irrigated zones) and maximum values of 0.018 (in dryland areas).

Boxplots and histograms indicated a right-skewed distribution of SbAI values, reinforcing the presence of a concentrated number of high-vulnerability pockets. Furthermore, a positive correlation ( $R^2 = 0.62$ ) was observed between high SbAI values and low NDVI zones, affirming that arid areas experience reduced vegetation vigor and likely reduced crop productivity. This supports the physical interpretation of SbAI as a surface dryness indicator impacting vegetation growth.

## 4.4. Comparison with Ground Truth and Agricultural Trends

The SbAI-derived vulnerability map was validated against ground survey data collected during field visits and from Mandya District Agricultural Office reports. Villages reporting frequent crop failures, poor soil moisture retention, and dependence on rain-fed agriculture aligned well with high SbAI values. Additionally, temporal crop yield data (especially for ragi, pulses, and sugarcane) showed a declining trend in high-SbAI zones, strengthening the argument that increasing aridity is having tangible impacts on agricultural productivity and rural livelihoods.

Farmers from Malavalli, Maddur, and Nagamangala reported perceptible changes in rainfall onset, longer dry spells, and increased dependence on borewell irrigation, many of which corroborate the satellite-observed increase in surface dryness and LST values. This alignment between remote sensing data and local perceptions enhances the credibility of SbAI as a decision-support indicator for climate adaptation.

#### 4.5. Implications for Policy and Climate Adaptation

The findings of this study hold significant implications for district-level climate resilience planning. By identifying village-level aridity hotspots, the study provides an evidence-based framework for targeted interventions such as rainwater harvesting, promotion of drought-tolerant crops, and groundwater recharge programs. The use of satellite-derived indices like SbAI enables cost-effective, scalable, and regularly updatable monitoring systems, especially in regions where field-based climate monitoring is logistically or financially constrained.

Furthermore, the integration of SbAI with socio-economic indicators such as landholding size, irrigation access, and cropping intensity in future assessments can lead to more holistic vulnerability mapping. The spatial tools developed through this research can be utilized by local agricultural departments, climate cells, and NGOs for micro-level planning and decision-making.

#### 4.6 Spatial Distribution of NDVI (2021)

The spatial distribution of NDVI values in 2021 across Mandya district exhibited a distinct contrast between irrigated command areas and rainfed uplands. NDVI values ranged from 0.18 to 0.62, with higher values indicating dense and healthy vegetation. The western and central taluks—notably Srirangapatna, Mandya, and Pandavapura—recorded NDVI values  $> 0.5$ , attributed to canal irrigation from the Cauvery River and double-cropping systems.

In contrast, Malavalli, Maddur, and parts of Nagamangala taluks showed NDVI values below 0.3, denoting sparse vegetation and degraded cropland, often associated with climatic stress, soil degradation, and water scarcity. These areas also overlap with known non-command zones where agriculture is highly dependent on monsoon rainfall.

#### 4.8 Temporal NDVI Trends: 2001 to 2021

Long-term NDVI analysis from 2001 to 2021 indicates a declining trend in average vegetation greenness across the district. The mean NDVI dropped from 0.48 in 2001 to 0.39 in 2021, suggesting increasing stress on vegetation due to rising temperatures, erratic rainfall, and shifting cropping patterns. The most significant declines were observed in rainfed areas, with Malavalli taluk registering a 20–25% drop in average NDVI over the 20-year period.

The decline in NDVI values aligns with observed climate anomalies, including frequent drought years (2002, 2012, and 2017) and extended dry spells during the kharif season. The impact is more pronounced in areas with sandy loam soils, shallow groundwater tables, and poor access to irrigation infrastructure.

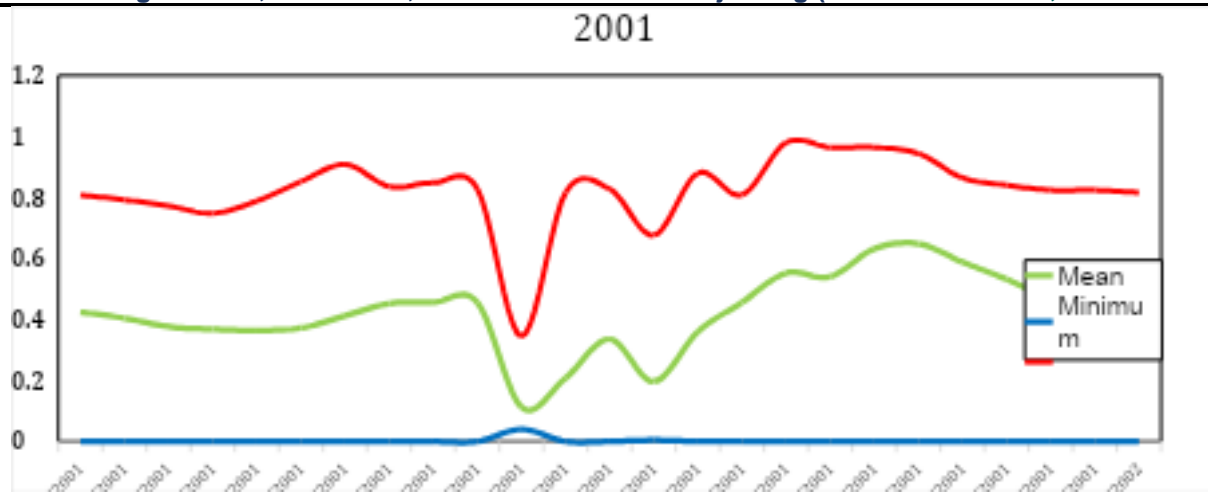


**Figure 4:** NDVI statistics of Mandya for the year 2001

#### 4.9. NDVI and Agricultural Vulnerability

A strong spatial correlation was observed between low NDVI zones and high agricultural vulnerability, based on ground reports of crop failure, reduced sowing area, and increased fallow land. These zones also exhibit low vegetation recovery even in normal rainfall years, indicating structural degradation of the agro ecosystem.

Additionally, NDVI anomalies for selected years (such as 2015 and 2020) showed negative departures from the mean, highlighting increased interannual variability in vegetation growth. These trends reflect the growing unpredictability of climatic conditions and suggest an urgent need for adaptive agricultural strategies in high-risk taluks.

### 5. Conclusion

The present study underscores the value of geospatial tools in assessing agricultural vulnerability to climate change, with a focused application in Mandya district, Karnataka. Using multi-temporal NDVI data derived from MODIS (2001–2021), the research identified critical spatial and temporal patterns in vegetation health that are indicative of underlying climatic stress. Areas under rainfed agriculture, especially in the eastern and southern taluks like Malavalli and Maddur, consistently exhibited lower NDVI values and more significant declines over time, reflecting both biophysical vulnerability and inadequate adaptive capacity.

The observed decline in vegetation greenness over the past two decades, coupled with spatial disparities in NDVI, signals increasing agricultural risk in the region. These findings align with broader climate change impacts such as erratic monsoons, rising temperatures, and frequent droughts, which disproportionately affect already fragile farming systems. Integrating satellite-based indicators like NDVI into vulnerability assessments allows for a cost-effective, data-driven, and spatially explicit approach to inform policy and planning.

In conclusion, this study provides vital evidence for identifying climate-sensitive zones within Mandya and recommends that district-level agricultural planning should prioritize these vulnerable areas for interventions such as climate-resilient cropping systems, micro-irrigation, and soil conservation. Further integration of NDVI with other indices such as the Satellite-based Aridity Index (SbAI) and socio-economic parameters can

enrich vulnerability models, offering comprehensive tools for adaptive agricultural management in a changing climate.

## References

- Adger, W. N. (2006). Vulnerability. *Global Environmental Change*, 16(3), 268–281. <https://doi.org/10.1016/j.gloenvcha.2006.02.006>
- de Sherbinin, A., Carr, D., Cassels, S., & Jiang, L. (2019). Population and environment. *Annual Review of Environment and Resources*, 34, 25.1–25.29.
- FAO. (2021). *The State of the World's Land and Water Resources for Food and Agriculture – Systems at breaking point*. Food and Agriculture Organization of the United Nations.
- Ghosh, S., Das, D., & Swain, M. (2021). Spatio-temporal assessment of climate vulnerability using remote sensing indicators in southern India. *Climate Risk Management*, 31, 100269.
- IPCC. (2014). *Climate Change 2014: Impacts, Adaptation, and Vulnerability*. Contribution of Working Group II to the Fifth Assessment Report of the Intergovernmental Panel on Climate Change. Cambridge University Press.
- IPCC. (2022). *Climate Change 2022: Impacts, Adaptation and Vulnerability*. Contribution of Working Group II to the Sixth Assessment Report of the Intergovernmental Panel on Climate Change. Cambridge University Press.
- Kogo, B. K., Kumar, L., & Koech, R. (2020). Climate change and variability in Kenya: A review of impacts on agriculture and food security. *Environment, Development and Sustainability*, 23, 23–43. <https://doi.org/10.1007/s10668-020-00589-1>
- Malczewski, J. (2006). GIS-based multicriteria decision analysis: A survey of the literature. *International Journal of Geographical Information Science*, 20(7), 703–726.
- Mondal, P., & Tatem, A. J. (2012). Uncertainty in measuring populations potentially impacted by sea level rise and coastal flooding. *PLoS ONE*, 7(10), e48191.
- Pandey, R., Jha, S. K., & Alatalo, J. M. (2019). Integrating climate change adaptation and disaster risk reduction into rural development: A case study from Himachal Pradesh, India. *Sustainability*, 11(13), 3735. <https://doi.org/10.3390/su11133735>
- Turner, B. L., Kasperson, R. E., Matson, P. A., et al. (2003). A framework for vulnerability analysis in sustainability science. *Proceedings of the National Academy of Sciences*, 100(14), 8074–8079.
- UNEP. (1992). *World Atlas of Desertification*. United Nations Environment Programme. Edward Arnold, London.
- You, Q., Min, J., Pepin, N. C., et al. (2020). Observed and projected trends in regional climate extremes and their impacts on crop production in China. *Science of The Total Environment*, 705, 135808.